Table 1 Configurations of the WRF physics schemes used in the present study.

Physical processes	Parameterization Scheme
Microphysics	Morrison 2-moment scheme (Morrison et al., 2009)
Long-wave radiation	RRTMG scheme (Iacono et al., 2008)
Short-wave radiation	RRTMG scheme
Surface layer	Monin-Obukhov scheme (Monin and Obukhov, 1954)
Land surface process	Noah land-surface model (Chen et al., 1996; Chen and Dudhia, 2001)
Planetary boundary layer process	Mellor-Yamada-Janjic TKE scheme (Mellor and Yamada, 1982; Janijic, 2001)

Table 2 Numerical experiments and corresponding urban land use and aerosol emissions.

Experiment	Land-use category	Anthropogenic emissions
LU06E06	2006	2006
LU70E06	1970	2006
LU70E70	1970	1970

Table 3 Analysis strategies for the investigation of urban land-use and/or aerosol effects.

Difference	Mechanism
LU06E06- LU70E06	Urban
LU70E06- LU70E70	Aerosol
LU06E06- LU70E70	Urban and aerosol

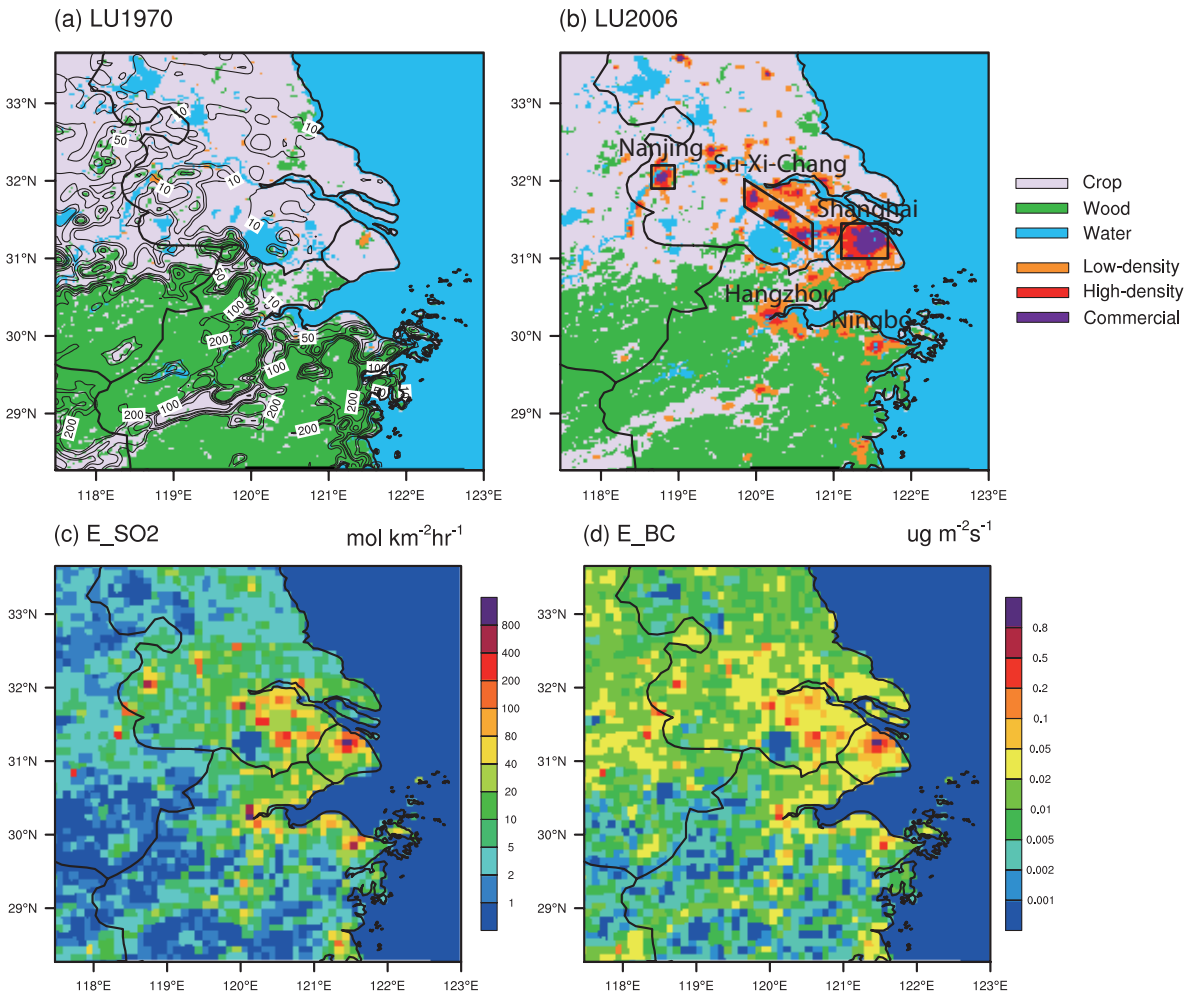

Figure 1 Land-use categories for year (a) 1970; (b) 2006; and (c) SO_2 (units: mol km^{-2} h^{-1}) and (d) black carbon (BC) emission rates (units: ug m^{-2} s^{-1}) averaged over 2006-2010. The topography is also shown in Fig. 1a (contour; units: m). The boxes in Fig. 1b outline three mega-city clusters of Nanjing, Su-Xi-Chang, and Shanghai.

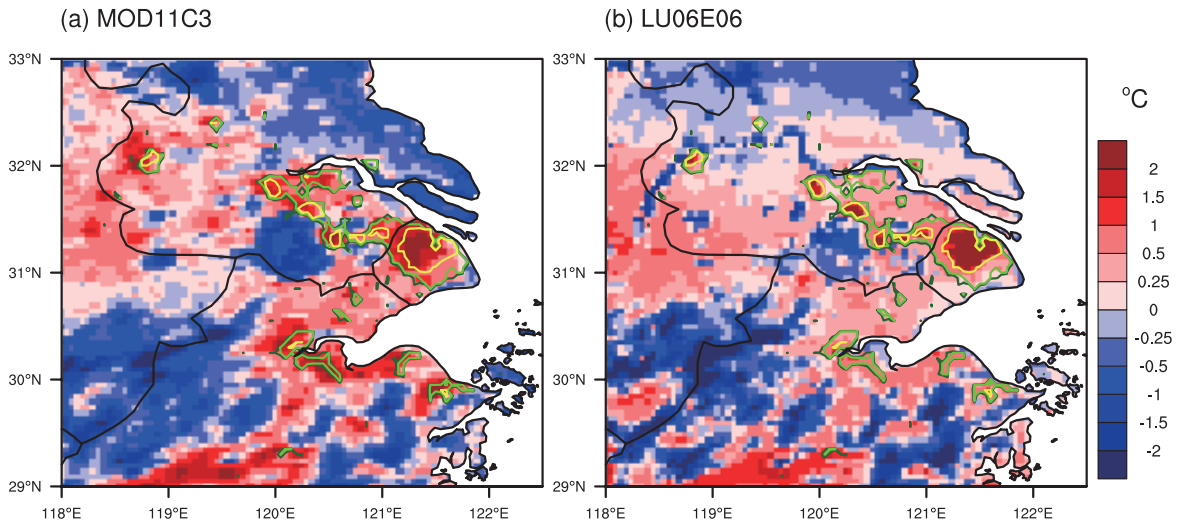

Figure 2 Moving spatial anomalies of averaged surface skin temperature (units: °C) with a filtering window size of 1° ×1° for (a) MODIS observation and (b) the L06E06 simulation. The "High Intensity Residential" and "Commercial/Industrial/Transportation" areas are marked with green lines and yellow lines, respectively.

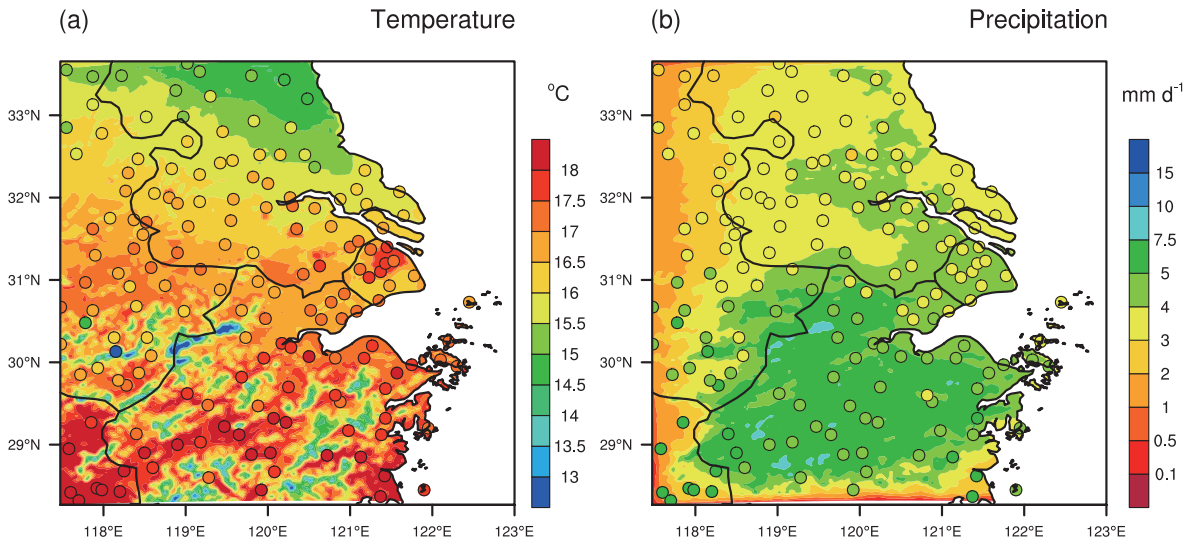

Figure 3 Annual mean (a) near-surface temperature (units: °C) and (b) precipitation (units: mm d^{-1}) from observations (shaded circles) and simulation of the LU06E06 (shaded).

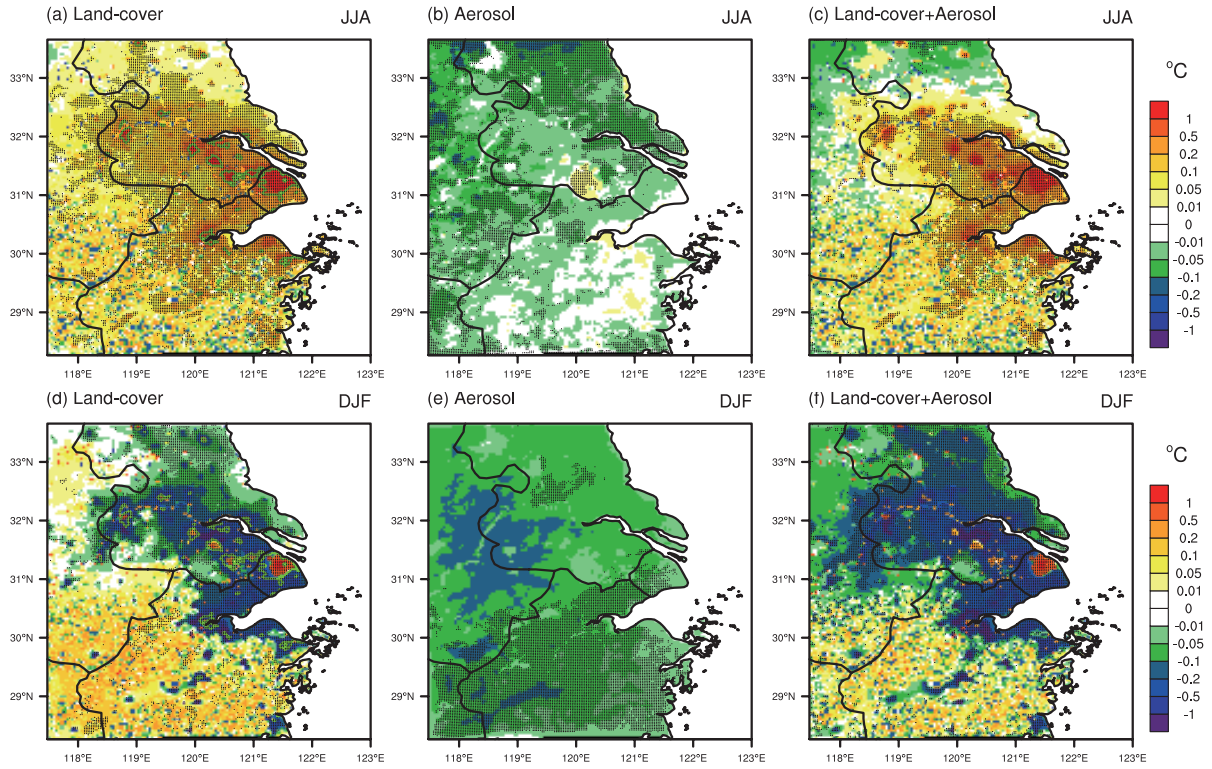

Figure 4 Differences in mean 2-m temperature (Units: °C) between simulations (a, d) LU06E70 and LU70E70, (b, e) LU70E06 and LU70E70, (c, f) LU06E06 and LU70E70 for summer (upper panels) and winter (bottom panels). "Commercial/Industrial/Transportation" areas are marked with green lines. The black dots mark the area with statistically significant changes.

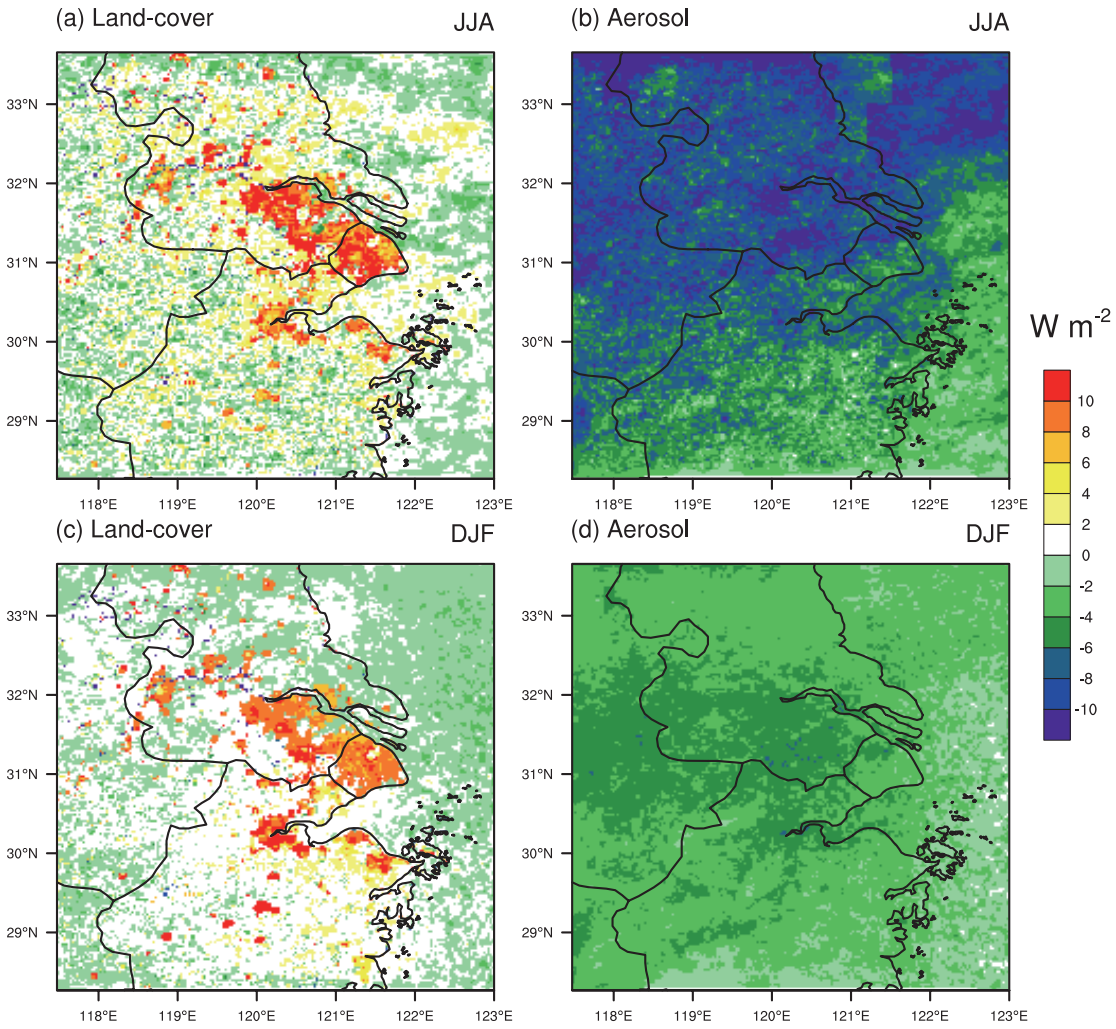

Figure 5 Differences in net shortwave fluxes at the surface (units: W m^{-2}) between simulations (a, c) LU06E70 and LU70E70, and (b, d) LU70E06 and LU70E70 in summer (upper panels) and winter (bottom panels).

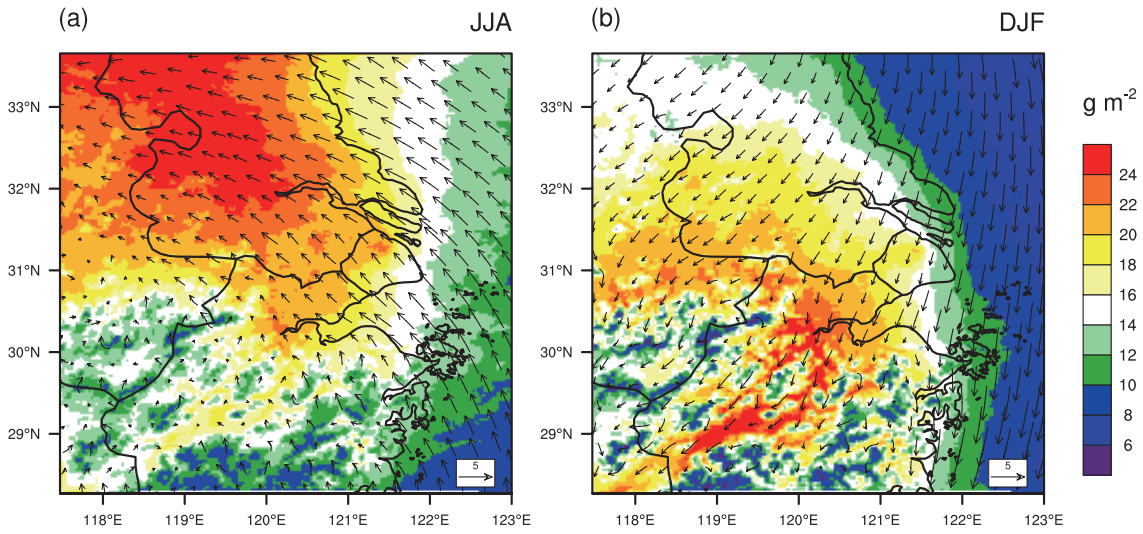

Figure 6 Differences in column burden of PM2.5 (g m^{-2}) between simulations LU70E06 and LU70E70, superimposed with near-surface winds simulated in LU70E70, for (a) summer and (b) winter.

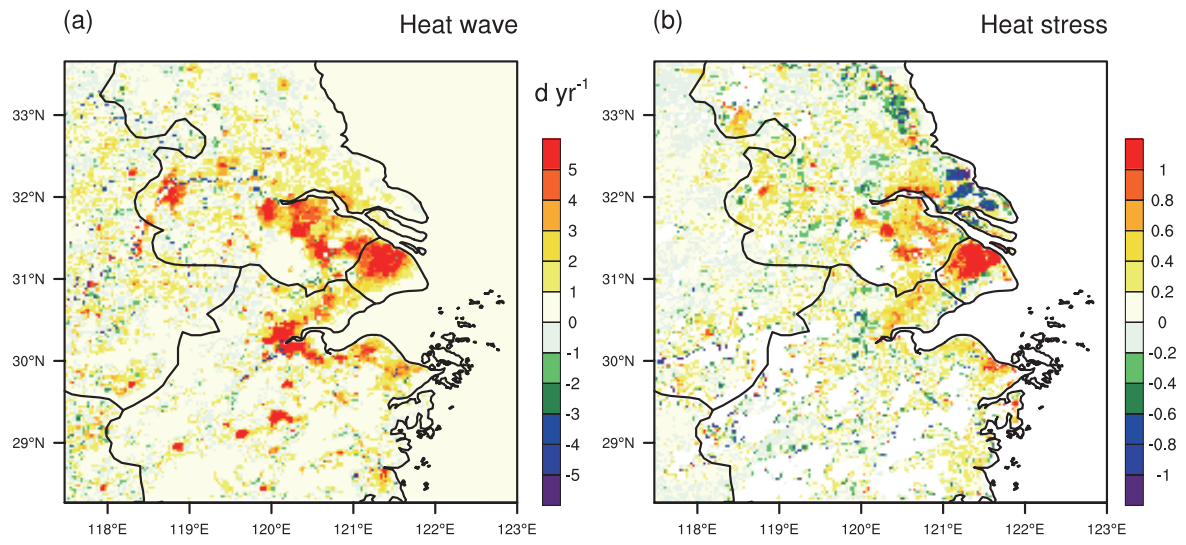

Figure 7 Differences in mean summertime (a) heat wave days (units: d/yr) and (b) heat stress (units: °C) between simulations LU06E70 and LU70E70.

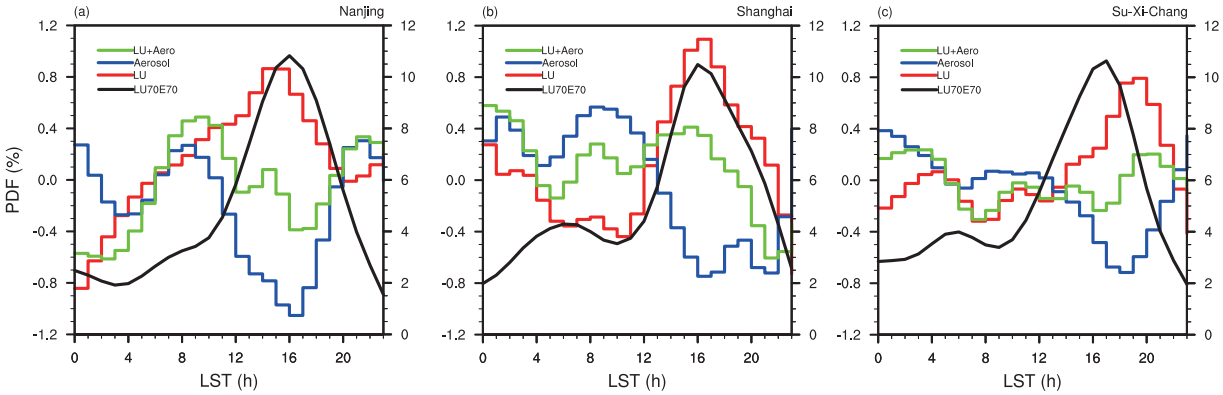

Figure 8 Diurnal cycles of the frequency of summertime extreme rainfall events for LU70E70 (defined using hourly precipitation intensity above 95th percentile, black lines, right axis) and the differences between simulations over (a) Nanjing, (b) Shanghai, and (c) Su-Xi-Chang. Red lines are for land use effect, blue lines for aerosol effect, and green lines for the combined effect.

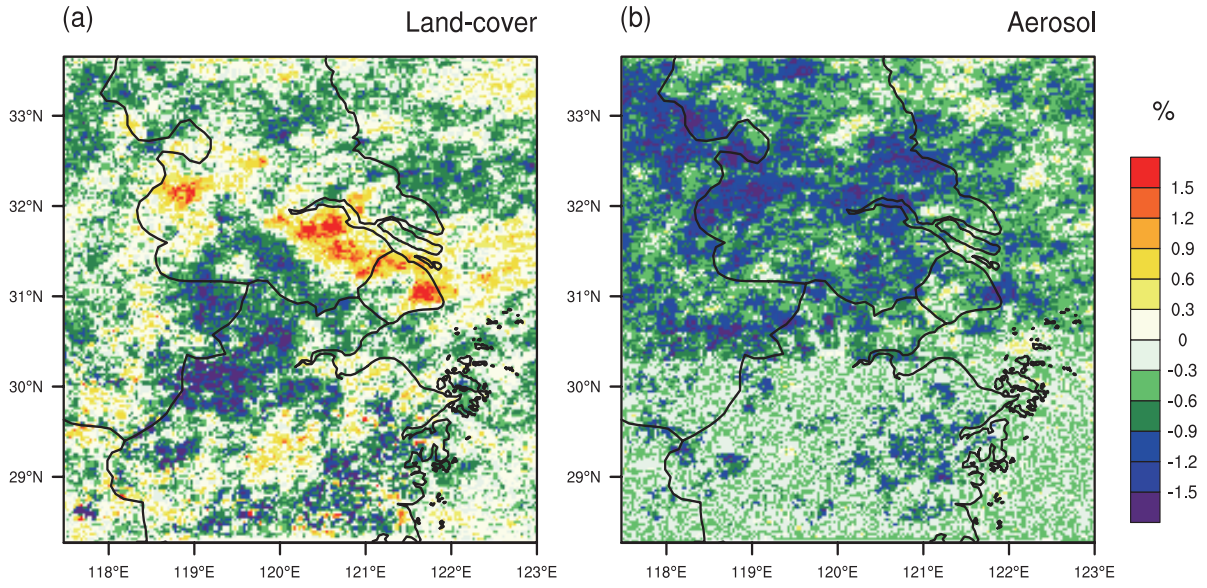

Figure 9 Differences in the frequency of summertime extreme rainfall events (averaged from 12:00 to 20:00 LST) between simulations (a) LU06E70 and LU70E70, and (b) LU70E06 and LU70E70.

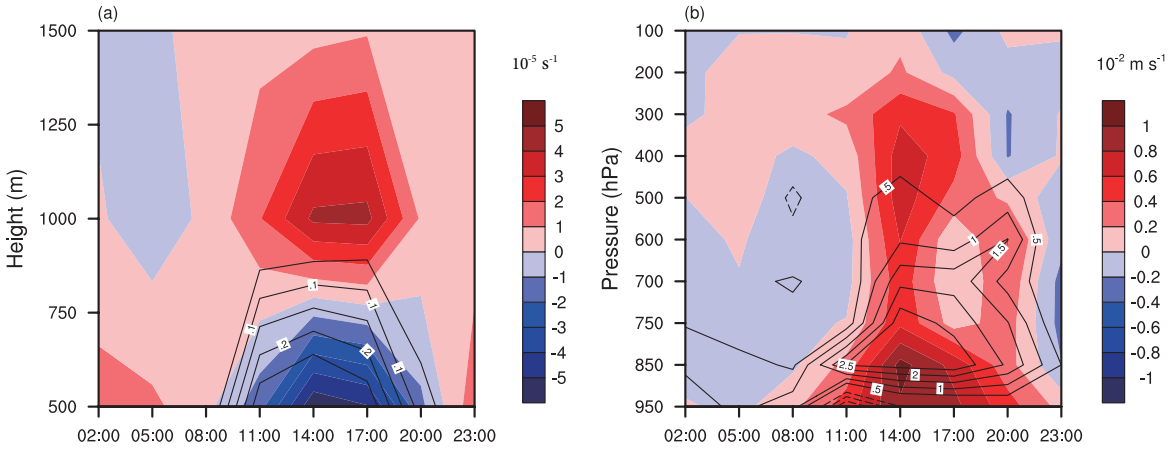

Figure 10 (a) Time-height cross-sections of differences (between LU06E70 and LU70E70) in temperature (contour; units: °C) and divergence (shade; units: 10^{-5} s^{-1}) averaged over the three city clusters (Nanjing, Shanghai, and Su-Xi-Chang); (b) same as (a), but for vertical velocity (shade; units: 10^{-2} m s^{-1}) and cloud water mixing ratio (contour; 10^{-3} kg kg^{-1}).

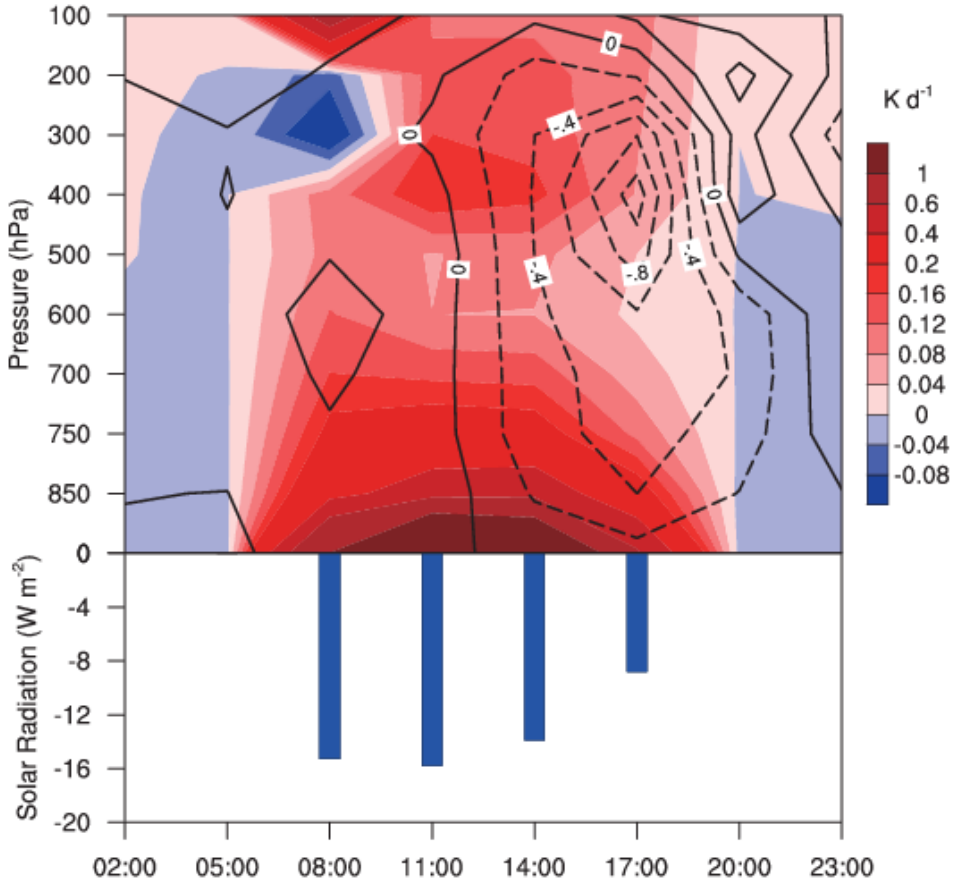

Figure 11 Time-height cross-sections of differences (between LU70E06 and LU70E70) in radiative heating profile (shade; units: K d^{-1}), vertical velocity (contour; units: 10^{-2} m s^{-1}) and surface solar radiation (blue bars; units: W m^{-2}) averaged over the three city clusters (Nanjing, Shanghai, and Su-Xi-Chang).

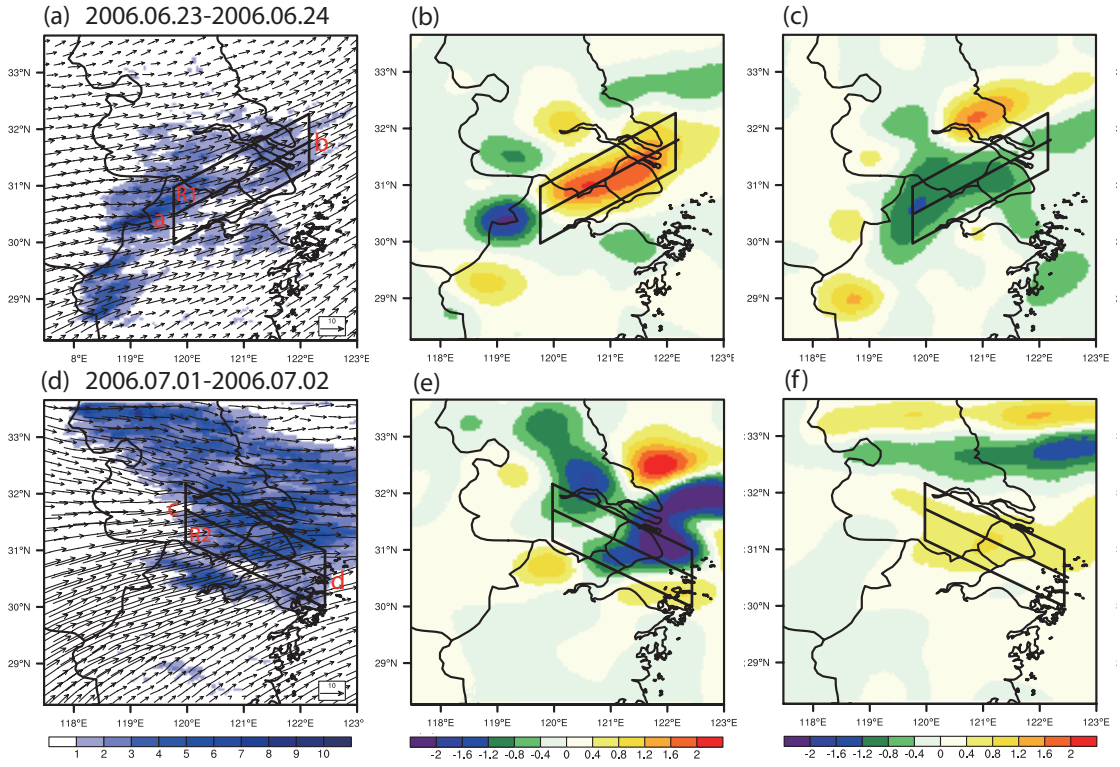

Figure 12 Rain rate (units: mm h-1) superimposed with wind vectors at 850 hPa for case A from 08:00 LST 23 June to 08:00 LST 24 June 2006 (a) simulated in the LU06E06 simulation, (b) differences between LU06E70 and LU70E70, (c) differences between LU70E06 and LU70E70. Panels (d-f) are the same as (a-c) but for case B from 08:00 LST 1 July to 08:00 LST 2 July 2006**.** The boxes R1 in (a), R2 in (d) outline the three regions over which further analysis are conducted. Lines across the center of each box mark the cross-sections to be analyzed.

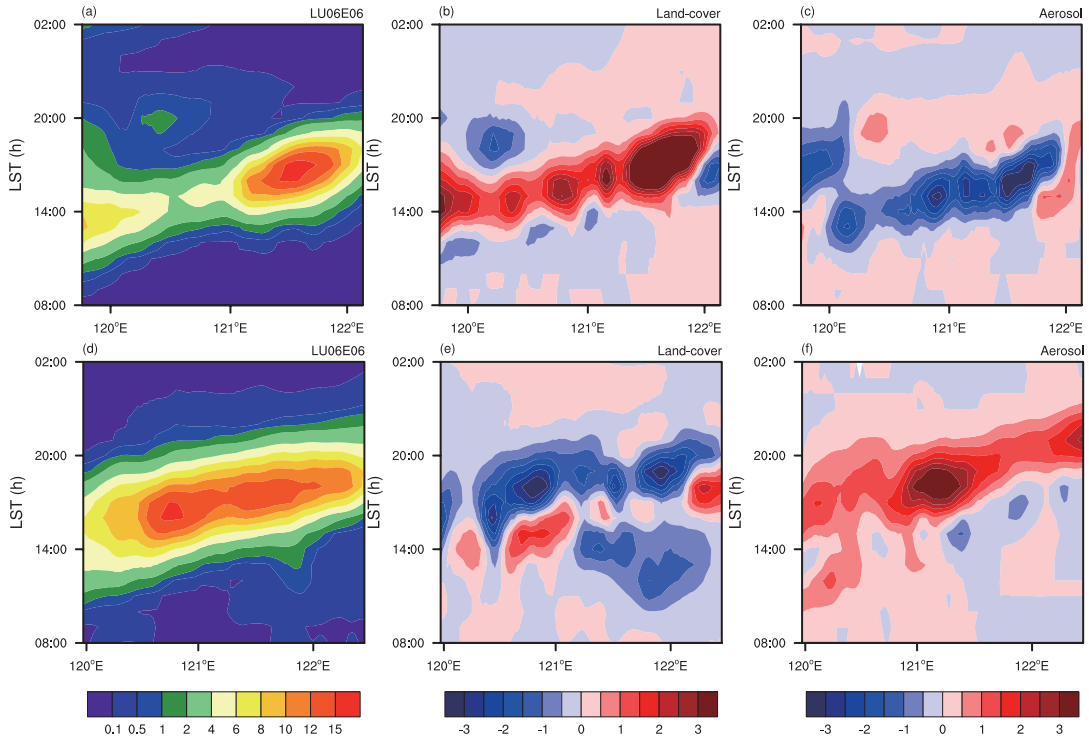

Figure 13 The time evolution of precipitation (units: mm h^{-1}) along the line *ab* (marked in Fig. 12a) from 08:00 LST 23 June to 02:00 LST 24 June 2006 (case A) (a) simulated in the LU06E06 simulation, (b) differences between LU06E70 and LU70E70, (c) differences between LU70E06 and LU70E70. Panels (d-f) are the same as (a-c) but for case B along line *cd* (marked in Fig. 12d) from 08:00 LST 1 July to 02:00 LST 2 July 2006**.**

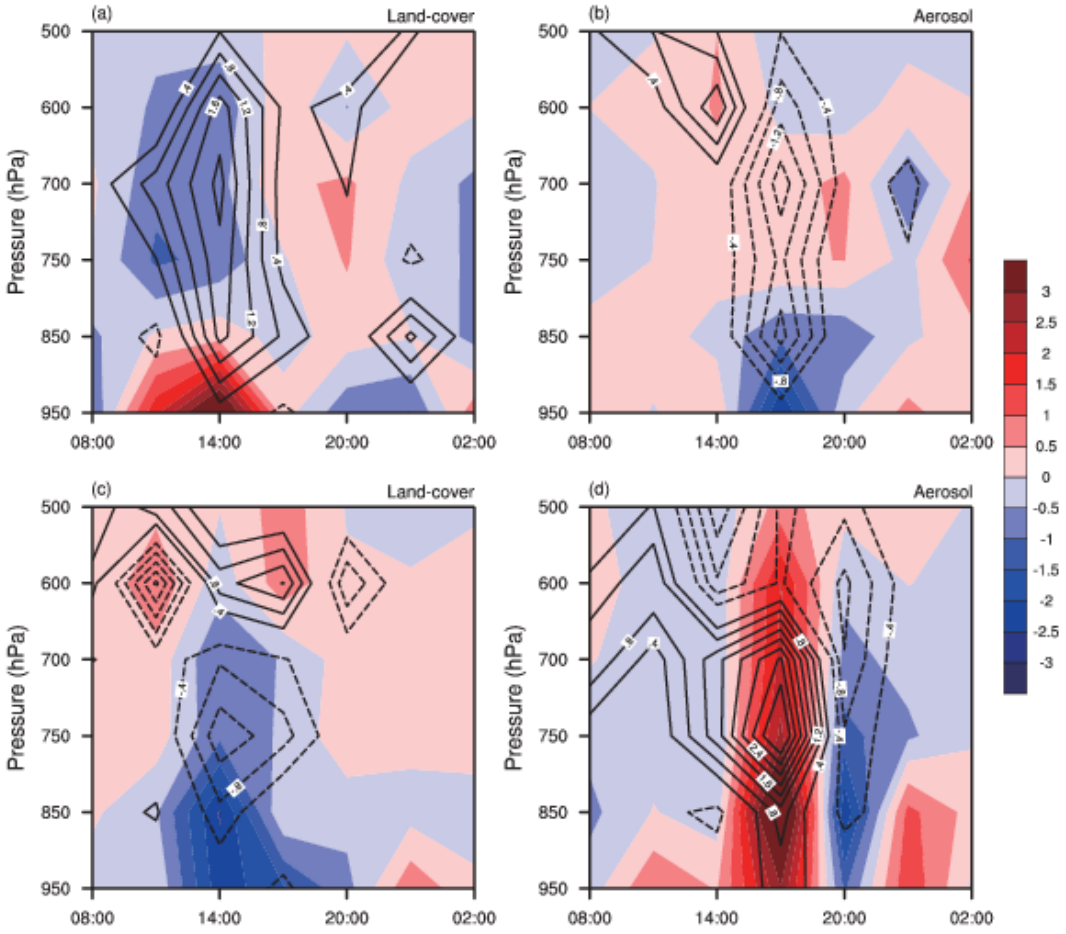

Figure 14 Time-height cross-sections of differences in moisture flux convergence (shaded; units: 10^{-4} g^{-1} kg^{-1} s^{-1}) and water vapor mixing ratio (black lines; units: 10^{-2} g kg^{-1}) from 08:00 LST 23 June to 02:00 LST 24 June 2006 (case A) over region R1 (denoted in Fig. 12a) between (a) LU06E70 and LU70E70; (b) LU70E06 and LU70E70; Panels (c, d) are the same as (a, b) but for case B from 08:00 LST 1 July to 02:00 LST 2 July 2006 over R2 (denoted in Fig. 12d).

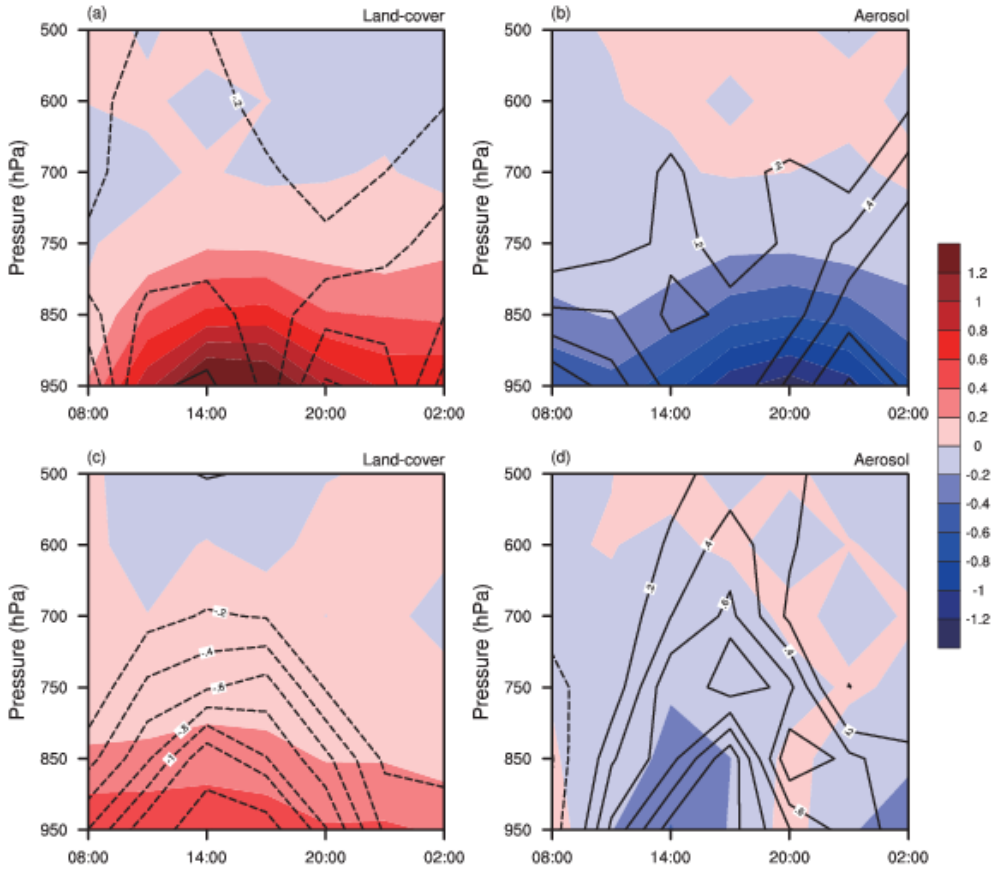

Figure 15 Same as Fig. 14 but for differences in the CON term (shaded; units: 10^{-4} $g^{-1}kg^{-1}$ s^{-1}) and MA term (black lines; units: 10^{-4} g^{-1} kg^{-1} s^{-1}) in eq. (2).

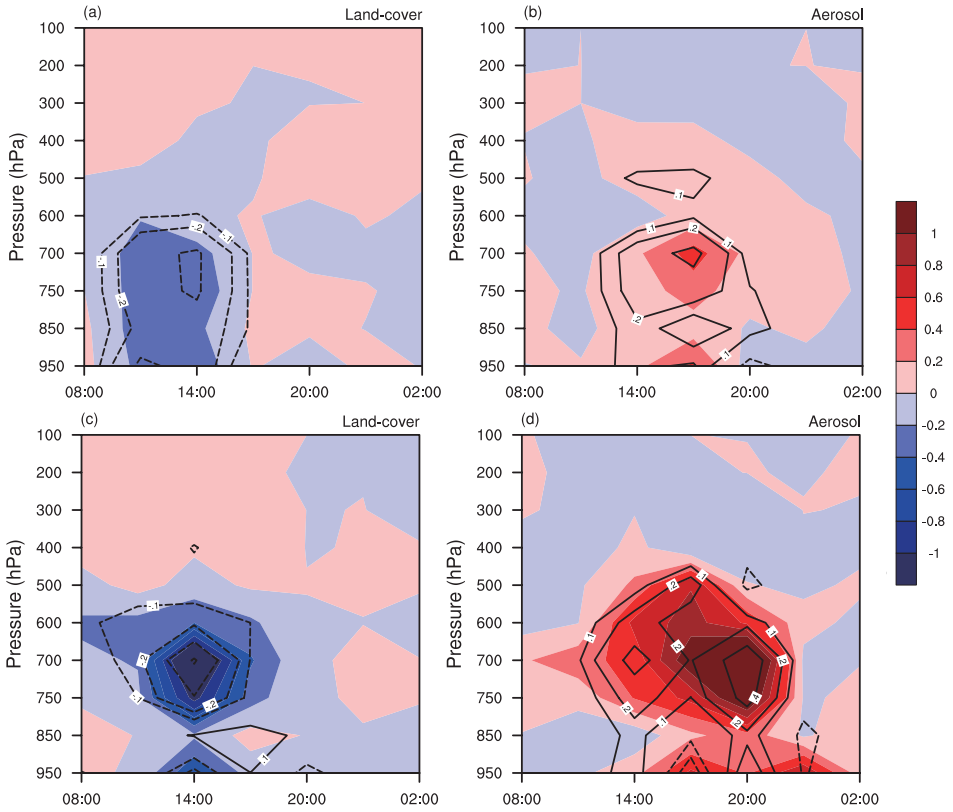

Figure 16 Same as Fig. 15 but for differences in the first term ($-V_{ctrl} \cdot \Delta(\nabla q)$) (shaded; units: 10^{-4} g^{-1} kg^{-1} s^{-1}) and the second term ($-(\nabla q)_{ctrl} \cdot \Delta V$) (black lines; units: 10^{-4} g^{-1} kg^{-1} s^{-1}) in Eq.3.